Experimental Investigation of Decoupling Effect on the Nonlinearity of Power Amplifiers in Transmitter Array

Fangyun Peng[1], Fei Yang[2], Bo Liu[1], and Xiaoming Chen[1]

[1]School of Information and Communications Engineering
Xi'an Jiaotong University, Xi'an, 710049, China
pfy2014111731@stu.xjtu.edu.cn, liuboright@stu.xjtu.edu.cn, xiaoming.chen@mail.xjtu.edu.cn

[2]China Academy of Space Technology
Xi'an, 711049, China
yfxjtu@163.com

Abstract – In a practical compact massive multiple-input multiple-output (MIMO) transmitter array, each antenna or subarray is connected to an independent power amplifier (PA) with a modest power capacity in order to avoid the challenging demand of high-power capacity of a single PA for the whole array and to facilitate the power dissipation of the transmitter array. In this case, there is simply not enough space for an isolator between the antenna and the PA. As a result, the array mutual coupling changes the load impedances of the PAs and thus further increases the MIMO transmitter's nonlinearity. In this work, the decoupling effect on the transmitter array's linearity is investigated experimentally by using an array prototype with PAs. The mutual coupling of the array can be effectively suppressed using a hybrid decoupling structure. Two continuous-wave (CW) signals at different frequencies are injected into the PAs, and the output signal of each PA is measured via a coupler. The measured results show that with effective mutual coupling reduction, the PA interference is greatly suppressed by up to 16 db and the amplitude of the desired signal is enhanced by up to 10 db.

Index Terms – mutual coupling, nonlinearity, power amplifier, transmitter array.

I. INTRODUCTION

The massive multi-input multi-output (MIMO) has been one of the key enablers for current and future wireless communications [1], [2]. Reduction of the power consumption and improvement of the transmitter linearity in a massive MIMO system has become a research hotspot. By configuring a large number of channels and antenna elements, the massive MIMO technique brings great performance enhancement, yet also introduces many thorny problems. Among them, the problem of nonlinear distortion of the power amplifiers (PAs) is particularly prominent [3–6]. The PAs are important modules in a MIMO transmitter array. In a practical MIMO transmitter array, each antenna or subarray is connected with an independent power amplifier (PA) with a modest power capacity instead of using a single PA with high-power capacity to feed the whole array. In this way, the transmitter can be more robust and cost-effective, and the multi-PA scheme also facilitates the power dissipation in the transmitter front-end. Moreover, for a compact massive array, there is not enough space for an isolator between the antenna and the PA. As a result, the mutual couplings between the elements in a MIMO array will change the active port impedance, resulting in mismatch between the antenna and the PA. In the presence of mutual coupling, the outputs of the PAs will interfere with each other, increasing the nonlinearity of the PA.

Figure 1 shows a schematic model of a MIMO transmitter array with PAs. Each element in the array is connected with a PA. The incident wave in the i-th PA ($a_{2,i}$) is dependent on the mutual couplings between antenna elements and the reflected wave in j-th PA ($b_{2,j}$), as mathematically described in (1). In other words, the mutual coupling changes the load impedances of the PAs, resulting in deteriorations of the PA efficiency and linearity.

$$a_{2,i} = \sum_{j=1}^{N} S_{i,j} b_{2,j}, \tag{1}$$

where the $s_{i,j}$ is the S-parameter between i-th and j-th element.

Various PA behavior models have been proposed to optimize the linearity [7] where the PA parameters are characterized by signal-tone or multi-tone excitation in measurements [8], [9]. A DC behavior was extended to a PA model [5] to predict the linearization and efficiency of PA in the presence of mutual coupling. A 4×1 array with 4 PAs was designed in [6], and the spectral results at the PA output were given to show the spectral regrowth with/without mutual coupling. Nonlinear

Submitted On: June 14, 2022
Accepted On: July 22, 2022

https://doi.org/10.13052/2023.ACES.J.380102

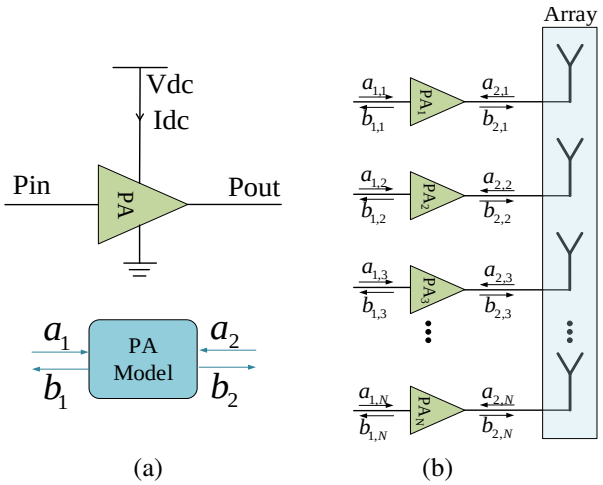

Fig. 1. Schematics of (a) a PA model with incident and reflected waves, and (b) N-element array with PAs.

distortion in phased-array transmitters was investigated in [10], simulated results therein showed that the main beam in-band distortion varies strongly with the steering angle in the presence of mutual coupling. The studies mentioned above only presented or predicted the nonlinear effect of mutual coupling on PA in transmitter arrays, without discussion on how to correct the distortions. A four-branch transmitter prototype was used in [11] to compare the spectrum distortion. It was reported that the regular linearization technique was ineffective to compensate the distortion due to the array mutual coupling. Instead of designing linearization techniques with high complexity, a cost-effective solution is to decouple the array from the antenna point of view. However, the decoupling effect on the linearity of the transmitter array has not been investigated yet.

In this paper, an antenna array prototype with a removable decoupling structure is connected with PAs. The PA output signals with and without array decoupling are measured. The experimental results show that the mutual coupling not only deteriorates the linearity but also creates strong interference. More importantly, it is shown that with effective array decoupling, both interference and spurious signals are greatly suppressed, and the desired signal is enhanced. To the best knowledge of the authors, this is the first experimental work demonstrating the decoupling effect on the linearity of a transmitter array.

II. COUPLING SUPPRESSION IN MIMO ARRAY

The MIMO array used in the test is a 4×4 base station (BS) array with a 57-mm horizontal inter-element spacing ($0.38\lambda_0$, where λ_0 is the free space wavelength at center frequency of 2.0 GHz) and a 117-mm vertical inter-element spacing ($0.75\lambda_0$). The four dual-polarized elements in each array column are combined using a power divider into one subarray with two antenna ports (for the $\pm 45^\circ$ polarizations), which is a typical BS array configuration.

The array has an operation band of 1.7-2.2 GHz. Due to the close horizontal inter-subarray spacing, the array suffers mutual coupling up to -15 db. Different decoupling techniques have been reported in previous works, e.g., decoupling metasurfaces [12–14], decoupling resonators [15], defected ground structure [16], and dielectric decoupling superstrate [17–19]. In order to increase the decoupling bandwidth, a hybrid decoupling method has been designed to reduce the mutual couplings down to -30 db at the center frequency. Figure 2 shows the coupling wave and decoupling mechanism between a two-element array. As shown in Fig. 2 (b), both the neutralization board and metal baffle are applied to the array. The neutralization board is suspended above the antenna to produce a reflective wave that is opposite in phase to the coupling wave, reducing the mutual coupling between elements. The metal baffle is placed between the two antennas to suppress the propagation of the space electromagnetic wave. Detailed description about the BS array and the decoupling method can be found in [19].

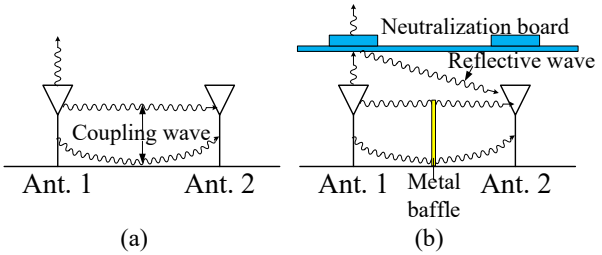

Fig. 2. Coupling wave between two-element array. (a) Array without decoupling and (b) with decoupling.

In order to realize the overall isolation enhancement of the MIMO array, a frequency domain solver based on finite element method (FEM) in an electromagnetic simulator CST 2020 [20] is used to design and optimize the array and decoupling structure. After the optimization of isolation, the array with removable decoupling structures are fabricated, as shown in Fig. 3.

This proposed decoupling method applies the combination of a metal baffle and the neutralization dielectric to the MIMO antenna array, which, compensating the insensitivity of the neutralization method to the cross-polarization coupling [21], significantly broadens the decoupling bandwidth of the compact, large-scale array. Figure 4 shows the simulated and measured S-parameters before and after decoupling. It can be seen

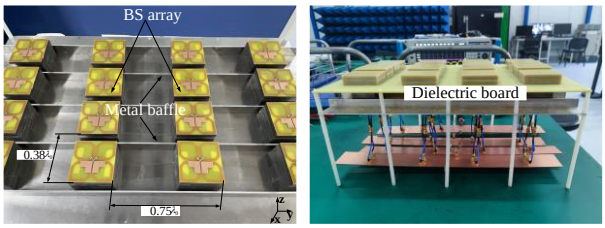

(a) (b)

Fig. 3. (a) Photograph of fabricated array with metal baffle. (b) Fabricated array with baffle and dielectric board.

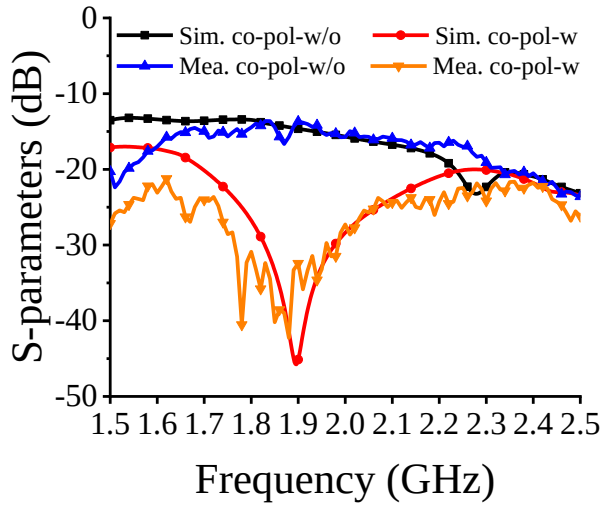

(a)

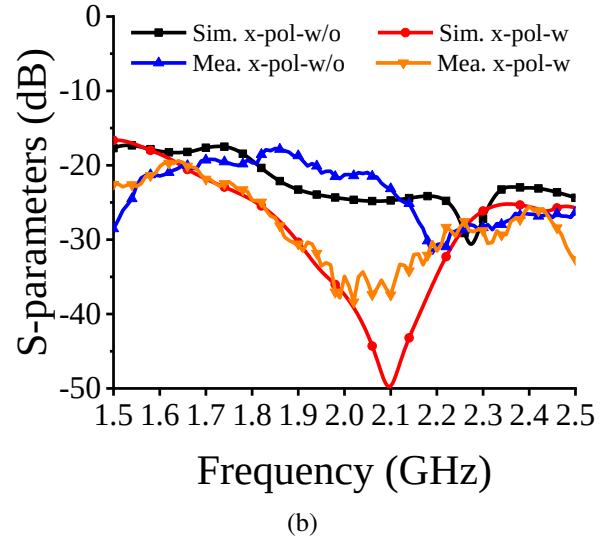

(b)

Fig. 4. Simulated and measured S-parameters before and after decoupling between antennas. (a) Co-polarized (co-pol) coupling. (b) Cross-polarized (x-pol) coupling.

that both the co-polarization and cross-polarization coupling between adjacent antennas (subarrays) has a significant reduction across the whole frequency band. The mutual couplings between adjacent elements are reduced to below −20 db within 1.7-2.2 GHz, and the couplings at the center frequency point are less than −30 db with a reduction of 15 -dB.

III. MODEL DESCRIPTION OF POWER AMPLIFIER

Figure 5 shows the configuration of the PA module used in the experimental test. This PA module contains two identical PA channels, i.e., channel A and channel B. Each channel includes a coupled port at the PA output. The coupled port can be considered as a coupler, whose power is about 40 db lower than that of the output. The signal characteristics of the PA's output can be inferred by observing the output signal from the coupled port.

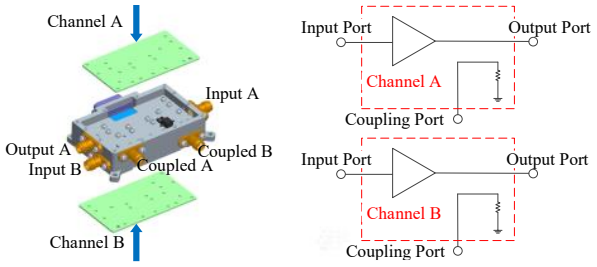

(a) (b)

Fig. 5. Configuration of the PA module. (a) 3-D view. (b) Schematic view.

The output load-pull impedance of the PA and the corresponding waveform are shown in Figs. 6 (a) and (b), respectively. The parasitic parameters of the transistor are de-embedded during simulation and test, which means that the results are obtained from the intrinsic current source plane (I_{gen} plane). The PA is biased with a gate voltage (VGS) of −3.2 V, corresponding to a Class-F condition. The drain voltage (V_{DS}) is 10 V. The fundamental impedance of $Z(f_0)$ is kept within nearly 50 Ohms from 2.03 GHz to 2.17 GHz, the corresponding second harmonic impedance $Z(2f_0)$ and the third harmonic impedance $Z(3f_0)$ are located at short and open, respectively, as shown in Fig. 6 (a). Under these impedances matching conditions, the drain voltage is approximately square wave, and the drain current is nearly half-wave rectified sinusoidal, which verifies the operation as Class-F mode [22], as shown in Fig. 6 (b). The measured results of the PA are shown in Figs. 6 (c) and (d). From 2.03 GHz to 2.17 GHz, the power added efficiency (PAE) is higher than 72%. The output power is larger than 30 dbm with a power gain larger than 11 -dB. Figure 6 (d) depicts the Pout, PAE and Gain performances within 10 -dB input-power range at the center

frequency of 2.1 GHz. The proposed PA is operating at the nearly P_{-3} point when P_{in}=20 dBm.

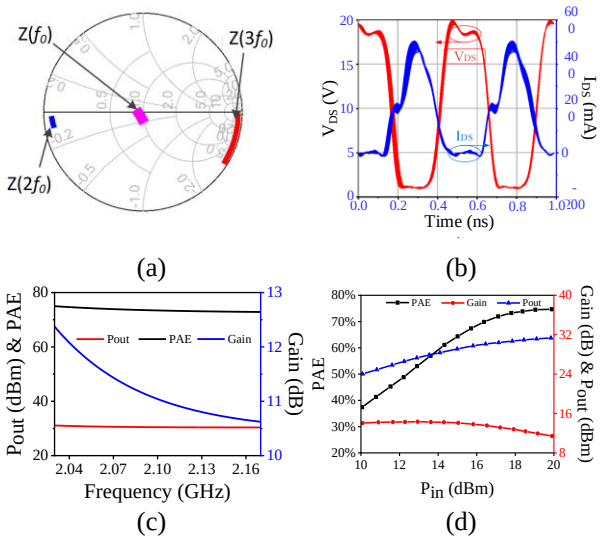

Fig. 6. (a) Output load-pull impedance. (b) Waveform in the I_{gen} plane. (c) Measurement results of the PA over frequency. (d) Measurement results of the PA over input power.

IV. MEASUREMENT SETUP AND RESULTS

A. Measurement setup

The BS array with and without the decoupling structure [19] is used to illustrate the decoupling effect on the linearity of the transmitter array. Two adjacent subarray ports of the same polarization are connected with two PAs (i.e., PA_1 and PA_2), while the rest of the subarray ports are terminated with 50-Ohm loads. Figure 7 shows the photo and schematic diagram of the measurement setup. Two continuous-wave (CW) signals with different frequencies from two signal generators are fed to the PAs. The PAs are fed by DC power supply where the DC voltage is 10 V. The coupled port of the PA is connected to a spectrum analyzer in order to observe the interference and nonlinearity of the PAs when loaded with the BS array with and without the decoupling.

The array without decoupling corresponds to the spectrum of high mutual coupling, and the array with decoupling corresponds to the spectrum of low mutual coupling.

Denote the two frequencies of the CW waves as f_1 and f_2, respectively. Three signal cases with different frequencies and amplitudes are used to illustrate the decoupling effect on the PA output spectrum.

Case 1: The input signal frequencies are set to f_1 = 2.05 GHz (inject to PA_1) and f_2 = 2.09 GHz (inject to PA_2) with 20-dBm amplitude.

Case 2: The input signal frequencies are set to $f1$ = 2.13 GHz (inject to PA_1) and f_2 = 2.08 GHz (inject to PA_2) with 15-dBm amplitude.

Case 3: The input signal frequencies are set to f_1 = 2.10 GHz (inject to PA_1) and f_2 = 2.13 GHz (inject to PA_2) with 10-dBm amplitude.

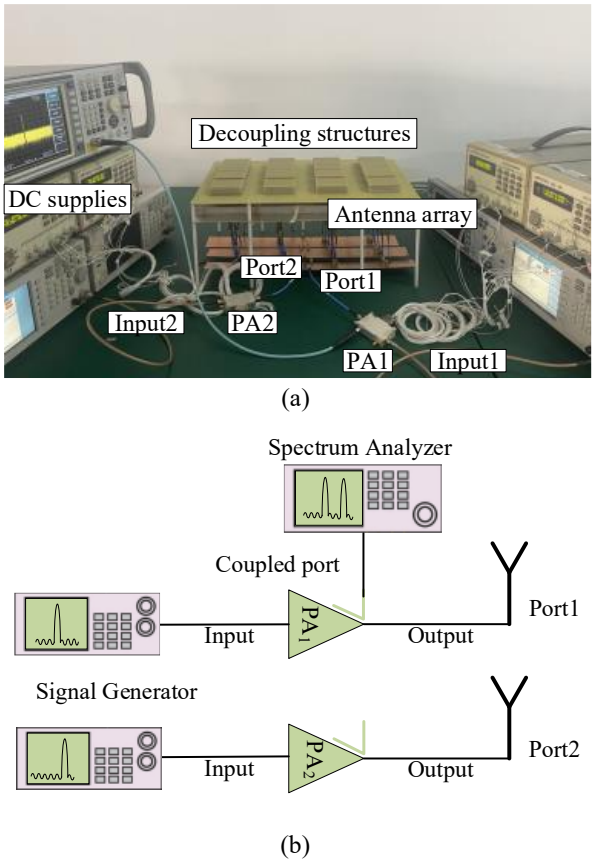

Fig. 7. (a) Photo and (b) schematic diagram of the measurement setup.

B. Measured Spectrum of PA

The PA_2 output spectra for case 1 with (wi. dec.) and without decoupling (w.o. dec.), are shown in Fig. 8 (a). If there were no mutual coupling or PA nonlinearity, the output spectrum from PA_2 should only contain the frequency of f_2 = 2.09 GHz. In the presence of mutual coupling and PA nonlinearity, however, the output spectrum from PA_2 contains multiple frequencies, as shown in Fig. 8 (a). The interference signal at f_1 = 2.05 GHz with an amplitude of -21.8 dbm is mainly due to the array mutual coupling. In addition, two spurious signals at 2.13 GHz and 2.17 GHz are observed due to the PA nonlinearity in the presence of mutual coupling. After the decoupling structure [cf. Fig. 3] is applied to the BS array, the mutual coupling is reduced by 15 db (i.e., from

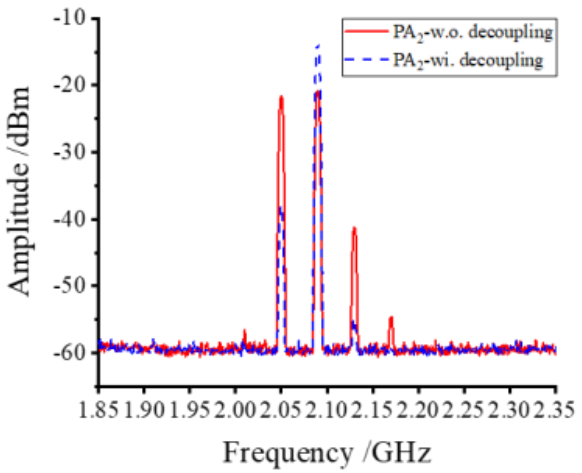

(a)

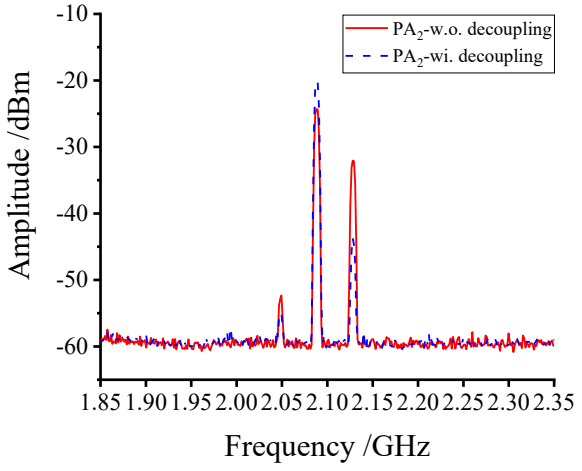

(b)

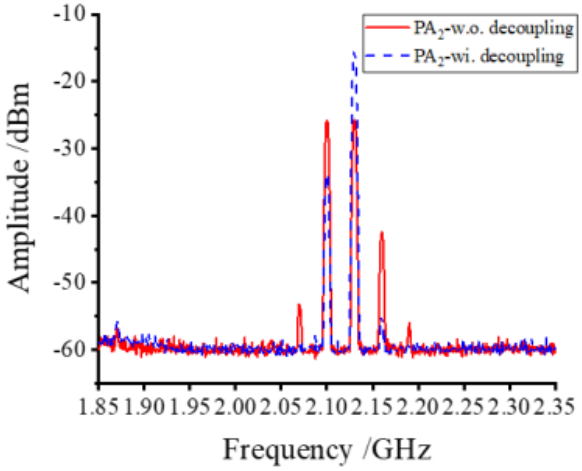

(c)

Fig. 8. Measured spectrum at the coupled port of PA_2 for (a) *case 1*, (b) *case 2* and (c) *case 3*.

−15 to −30 db). As a result, the interference signal at f_1 = 2.05 GHz is suppressed by 16.1 db (i.e., from −21.8 to −37.9 dbm), the two spurious signals at 2.13 GHz and 2.17 GHz are almost eliminated, and the useful signal at f_2 = 2.09 GHz (i.e., the input frequency) is increased from −21.0 to −14.2 dbm.

The PA_2 output spectrum for case 2 with and without decoupling are depicted in Fig. 8 (b). The results are consistent with that of case 1. The interference signal occurring at f_1 = 2.13 GHz is mainly due to the mutual coupling, while the spurious signal at 2.05 GHz is attributed to the combination of PA nonlinearity and mutual coupling. With effective decoupling, the interference signal at f_1 = 2.13 GHz is reduced from −32.1 dbm to −43.7 dbm, while the amplitude of the useful signal at f_2=2.08 GHz is improved from −24.2 to −20.1 dbm.

Figure 8 (c) depicts the PA_2 output spectrum of case 3 with and without decoupling, and the results of case 3 are consistent with that of case 1 and case 2. When the mutual coupling in array is significantly reduced, the interference and spurious caused by nonlinearity are suppressed, such as the interference signal at 2.10 GHz is reduced from −26.1 dbm to −33.8 dbm, the spurious signal at 2.16 GHz is almost completely eliminated, while the amplitude of the desired signal at f_2 = 2.13 GHz increases from −25.9 dbm to −15.6 dbm.

Table 1 summarizes the comparison of PA_2 output spectrum in the array with and without decoupling in three cases, all of which increase the desired signal amplitude and suppress interference and spurious signals.

Table 1: Comparison of PA_2 output after decoupling

	Case 1	*Case 2*	*Case 3*
Improvement of desired signal/dB	6.8	4.1	10.3
Suppression of interference /dB	16.1	11.6	7.7

Table 2: Suppression of PA_1 output at different amplitudes

	Case 1	Case 2	Case 3
Magnitude of CW signal /dBm	20	15	10
Suppression of interference /dB	7.7	9.6	7.6

The results in Table 1 are for PA_2. The output results of PA_1 are similar, as shown in Fig. 9. After the mutual coupling in the array is reduced, the output spectrum result of PA_1 is that the desired signal is enhanced and

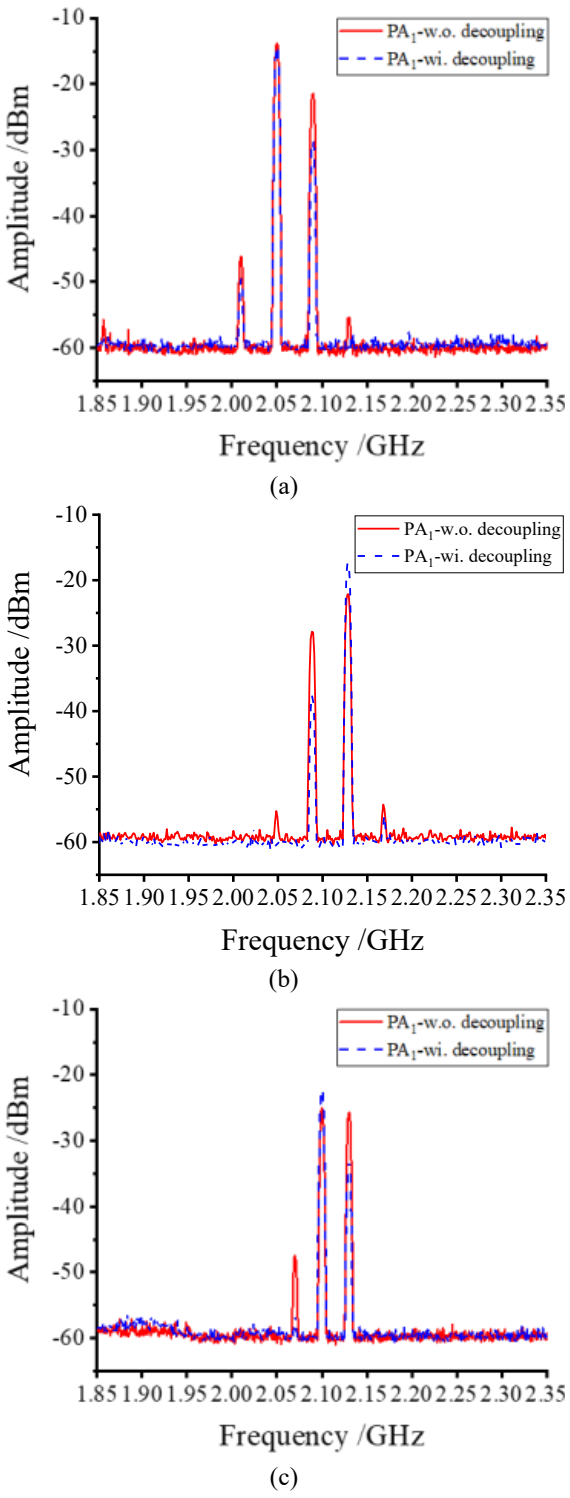

Fig. 9. Measured spectrum at the coupled port of PA_1 for (a) *case 1*, (b) *case 2* and (c) *case 3*.

the interfering signal is suppressed. Table 2 shows the the suppression level of interference signal for different amplitudes. When the amplitude of the input signal varies from 20 db to 10 db, the coupling reduction can bring obvious interference suppression effect.

V. CONCLUSION

A measurement-based characterization of the decoupling effect on the PA linearity in a transmitter array has been conducted in this paper. The experimental results show that the mutual coupling not only deteriorates the linearity, but also produces strong interference. For three cases with different frequencies and amplitudes, the desired signal could be improved by 4-10 db, and the spurious and interference signals could be suppressed by 7-16 db. It was demonstrated experimentally that decoupling could improve the PA linearity, reduce the interference, and enhance the desired signal in the transmitter array. Sci. China Inf. Sci.

ACKNOWLEDGEMENTS

This work was supported by the National Key R&D Program of China under Grant 2022YFB3902400.

REFERENCES

[1] H. Pei, X. Chen, X. Huang, X. Liu, X. Zhang, and Y. Huang, "Key issues and algorithms of multiple-input-multiple-output over-the-air testing in the multi-probe anechoic chamber setup," *Sci. China Inf. Sci.*, vol. 65, no. 3, pp. 47-73, Mar. 2022.

[2] R. He, B. Ai, G. Wang, M. Yang, C. Huang, and Z. Zhong, "Wireless channel sparsity: Measurement, analysis, and exploitation in estimation," *IEEE Wireless Commun.*, vol. 28, no. 4, pp. 113-119, Aug. 2021.

[3] B. Gashi, S. Krause, R. Quay, C. Fager, and O. Ambacher, "Investigations of active antenna doherty power amplifier modules under beam-steering mismatch," *IEEE Microwave Compon. Lett.*, vol. 28, no. 10, pp. 930-932, Oct. 2018.

[4] K. Hausmair, S. Gustafsson, C. Sánchez-Pérez, P. N. Landin, U. Gustavsson, T. Eriksson, and C. Fager, "Prediction of nonlinear distortion in wideband active antenna arrays," *IEEE Trans. Microwave Theory Tec.*, vol. 65, no. 11, pp. 4550-4563, Nov. 2017.

[5] F. M. Barradas, T. R. Cunha, P. M. Cabral, and J. C. Pedro, "Modeling PA linearity and efficiency in MIMO transmitters," *IEEE MTT S. Int. Microwave Sym. Dig.*, Honolulu, HI, USA, pp. 1999-2002, Oct. 2017.

[6] F. M. Barradas, P. M. Tomé, J. M. Gomes, T. R. Cunha, P. M. Cabral, and J. C. Pedro, "Power, linearity, and efficiency prediction for MIMO arrays with antenna coupling," *IEEE Trans. Microwave Theory Tech.*, vol. 65, no. 12, pp. 5284-5297, Nov. 2017.

[7] J. C. Pedro and S. A. Maas, "A comparative overview of microwave and wireless power-amplifier behavioral modeling approaches," *IEEE Trans. Microwave Theory Tech.*, vol. 53, no. 41, pp. 1150-1163, Apr. 2005.

[8] D. H. Wisell, B. Rudlund, and D. Ronnow, "Characterization of memory effects in power amplifiers using digital two-tone measurements," *IEEE Trans. Instrum. Mea.*, vol. 56, no. 6, pp. 2757-2766, Dec. 2007.

[9] S. Amin, W. Van Moer, P. Händel, and D. Rönnow, "Characterization of concurrent dual-band power amplifiers using a dual two-tone excitation signal," *IEEE Trans. Instrum. Mea.*, vol. 64, no. 10, pp. 2781-2791, Oct. 2015.

[10] C. Fager, K. Hausmair, K. Buisman, K. Andersson, E. Sienkiewicz, and D. Gustafsson, "Analysis of nonlinear distortion in phased array transmitters," *Proc. Int. Workshop Integr. Nonlinear Microw. Millimetre-Wave Circuits, INMMiC*, Graz, Austria, pp. 1-4, May 2017.

[11] C. Fager, T. Eriksson, F. Barradas, K. Hausmair, T. Cunha, and J. C. Pedro, "Linearity and efficiency in 5G transmitters: new techniques for analyzing efficiency, linearity, and linearization in a 5G active antenna transmitter context," *IEEE Microwave Mag.*, vol. 20, no. 5, pp. 35-49, May 2019.

[12] J. Jiang, Y. Li, L. Zhao, L. Zhao, and X. Liu, "Wideband MIMO directional antenna array with a simple meta-material decoupling structure for X-Band applications," *Applied Computational Electromagnetics Society (ACES) Journal*, vol. 35, no. 5, pp. 556-566, May 2020.

[13] J. Jiang, Y. Xia, and Y. Li, "High isolated X-Band MIMO array using novel wheel-like metamaterial decoupling structure," *Applied Computational Electromagnetics Society (ACES) Journal*, vol. 34, no. 12, pp. 1829-1836, 2019.

[14] X. Chen, M. Zhao, H. Huang, Y. Wang, S. Zhu, C. Zhang, J. Yi, and A. A. Kishk, "Simultaneous decoupling and decorrelation scheme of MIMO arrays," *IEEE Tran. Veh. Technol.*, vol. 71, no. 2, pp. 2164-2169, Feb. 2022.

[15] F. Faraz, X. Chen, Q. Li, J. Tang, J. Li, T. A. Khan, and X. Zhang, "Mutual coupling reduction of dual polarized low profile MIMO antenna using decoupling resonators," *Applied Computational Electromagnetics Society (ACES) Journal*, vol. 35, no. 1, pp. 38-43, 2020.

[16] B. Qian, X. Chen, and A. A. Kishk, "Decoupling of microstrip antennas with defected ground structure using the common/differential mode theory," *IEEE Antennas Wirel. Propag. Lett.*, vol. 20, no. 5, pp. 828-832, May 2021.

[17] Y. Da, Z. Zhang, X. Chen, and A. A. Kishk, "Mutual coupling reduction with dielectric superstrate for base station arrays," *IEEE Antennas Wirel. Propag. Lett.*, vol. 20, no. 5, pp. 843-847, May 2021.

[18] F. Liu, J. Guo, L. Zhao, G. Huang, Y. Li and, Y. Yin, "Ceramic superstrate-based decoupling method for two closely packed antennas with cross-polarization suppression," *IEEE Trans. Antennas Propag.*, vol. 69, no. 3, pp. 1751-1756, 2021.

[19] B. Liu, Y. Da, X. Chen, and A. A. Kishk, "Hybrid decoupling structure based on neutralization and partition schemes for compact large-scale base station arrays," *IEEE Antennas Wirel. Propag. Lett.*, vol. 21, no. 2, pp. 267-271, 2022.

[20] CST Microwave Studio, CST Gmbh, 2020. http://www.cst.com

[21] B. Liu, X. Chen, J. Tang, A. Zhang, and A. A. Kishk, "Co- and cross-polarization decoupling structure with polarization rotation property between linearly polarized dipole antennas with application to decoupling of circularly polarized antennas," *IEEE Trans. Antennas Propag.*, vol. 70, no. 1, pp. 702-707, Jan. 2022.

[22] D. Kang, D. Yu, K. Min, J. Choi, D. Kim, B. Jin, M. Jun, and B. Kim, "A highly efficient and linear class-AB/F power amplifier for multimode operation," *IEEE Trans. Microwave Theory Tech.*, vol. 56, no. 1, pp. 77-87, Jan. 2008.

Fangyun Peng received her B.Sc. degree in Electrical Information Engineering from Southwest Jiaotong University, Chengdu, China, in 2018. She is currently pursuing a Ph.D. degree at the School of Electronic and Information Engineering from Xi'an Jiaotong University. Her research interests include over-the-air testing.

Fei Yang is with the China Academy of Space Technology.

Bo Liu received his B.Sc. degree in Electronic Information Engineering from Xidian University, Xi'an, China, in 2019. He received his M.Sc. degree from the School of Electronic and Information Engineering, Xi'an Jiaotong University, Xi'an, China, in 2022. His research interests include MIMO antennas and the decoupling of MIMO antennas.

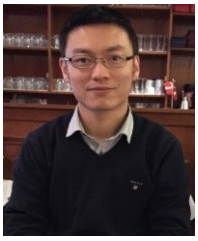

Xiaoming Chen received his B.Sc. degree in Electrical Engineering from Northwestern Polytechnical University, Xi'an, China, in 2006, and M.Sc. and Ph.D. degrees in Electrical Engineering from Chalmers University of Technology, Gothenburg, Sweden, in 2007 and 2012, respectively. From 2013 to 2014, he was a postdoctoral researcher at that same university. From 2014 to 2017, he was with Qamcom Research & Technology AB, Gothenburg, Sweden. Since 2017, he has been a professor at Xi'an Jiaotong University, Xi'an, China. His research areas include MIMO antennas, over-the-air testing, reverberation chambers and has published more than 150 journal articles on these topics.

Prof. Chen currently serves as a Senior Associate Editor for IEEE Antennas and Wireless Propagation Letters. He was the general chair of the IEEE International Conference on Electronic Information and Communication Technology (ICEICT) in 2021. He won the first prize of the universities' scientific research results in Shaanxi province, China, 2022. He received the IEEE outstanding Associate Editor awards in 2018, 2019, 2020, 2021, and the URSI (International Union of Radio Science) Young Scientist Award 2017 and 2018.